AFRL-AFOSR-VA-TR-2016-0262

Irregularties and Forecast Studies of Equatorial Spread

David Hysell
CORNELL UNIVERSITY
373 PINE TREE RD
ITHACA, NY 14850-2820

07/25/2016
Final Report

Air Force Research Laboratory
AF Office Of Scientific Research (AFOSR)/RTB1

Arlington, Virginia 22203
Air Force Materiel Command

REPORT DOCUMENTATION PAGE

Form Approved
OMB No. 0704-0188

1. REPORT DATE *(DD-MM-YYYY)*	2. REPORT TYPE	3. DATES COVERED *(From - To)*
25-07-2016	FinalPerformance	15 Sep 2012 to 14 Sep 2016

4. TITLE AND SUBTITLE
Irregularties and Forecast Studies of Equatorial Spread

5a. CONTRACT NUMBER

5b. GRANT NUMBER
FA9550-12-1-0462

5c. PROGRAM ELEMENT NUMBER
61102F

6. AUTHOR(S)
David Hysell

5d. PROJECT NUMBER

5e. TASK NUMBER

5f. WORK UNIT NUMBER

7. PERFORMING ORGANIZATION NAME(S) AND ADDRESS(ES)
CORNELL UNIVERSITY
373 PINE TREE RD
ITHACA, NY 14850-2820 US

8. PERFORMING ORGANIZATION REPORT NUMBER

9. SPONSORING/MONITORING AGENCY NAME(S) AND ADDRESS(ES)
AF Office of Scientific Research
875 N. Randolph St. Room 3112
Arlington, VA 22203

10. SPONSOR/MONITOR'S ACRONYM(S)
AFRL/AFOSR RTB1

11. SPONSOR/MONITOR'S REPORT NUMBER(S)
AFRL-AFOSR-VA-TR-2016-0262

12. DISTRIBUTION/AVAILABILITY STATEMENT
A DISTRIBUTION UNLIMITED: PB Public Release

13. SUPPLEMENTARY NOTES

14. ABSTRACT

Progress simulating equatorial spread F (ESF) in pursuit of a space-weather forecast capability is summarized. ESF is the main manifestation of space weather at low magnetic latitudes in the ionosphere and is responsible for disrupting communication, navigation, imaging, and surveillance systems important to the Air Force and other federal agencies.
A 3D numerical simulation of the plasma instabilities responsible for ESF written at Cornell has been developed and upgraded under this award. Plasma number density, electric field, and neutral wind data necessary for driving the simulation have been collected in campaigns at the Jicamarca Radio Observatory conducted approximately semi-annually. The simulation code is initialized and forced using campaign data. Simulation results, specifically the plasma depletions and plumes characteristic of ESF, are compared with coherent scatter radar imagery of ESF irregularities made at Jicamarca. Such imagery is directly comparable to the 3D simulation products, offering a prediction-assessment strategy that is uniquely conducive to closure. In multiple campaign studies, the simulation was able to recover the ionospheric dynamics that unfolded in nature including the occurrence or non-occurrence of ESF

15. SUBJECT TERMS
ionosphere irregularity, ionosphere modeling, equatorial spread F, forecasting, C/NOFS

16. SECURITY CLASSIFICATION OF:			17. LIMITATION OF ABSTRACT	18. NUMBER OF

Standard Form 298 (Rev. 8/98)
Prescribed by ANSI Std. Z39.18

a. REPORT	b. ABSTRACT	c. THIS PAGE		PAGES	19a. NAME OF RESPONSIBLE PERSON
Unclassified	Unclassified	Unclassified	UU		MOSES, JULIE
					19b. TELEPHONE NUMBER *(Include area code)* 703-696-9586

Final Report: Irregularties and Forecast Studies of Equatorial Spread *F* Grant/Contract Number: FA9550-12-1-0462

D. L. Hysell
Earth and Atmospheric Sciences
Cornell University

July 13, 2016

Abstract

Progress simulating equatorial spread F (ESF) in pursuit of a space-weather forecast capability is summarized. ESF is the main manifestation of space weather at low magnetic latitudes in the ionosphere and is responsible for disrupting communication, navigation, imaging, and surveillance systems important to the Air Force and other federal agencies.

A 3D numerical simulation of the plasma instabilities responsible for ESF written at Cornell has been developed and upgraded under this award. Plasma number density, electric field, and neutral wind data necessary for driving the simulation have been collected in campaigns at the Jicamarca Radio Observatory conducted approximately semi-annually. The simulation code is initialized and forced using campaign data. Simulation results, specifically the plasma depletions and plumes characteristic of ESF, are compared with coherent scatter radar imagery of ESF irregularities made at Jicamarca. Such imagery is directly comparable to the 3D simulation products, offering a prediction-assessment strategy that is uniquely conducive to closure. In multiple campaign studies, the simulation was able to recover the ionospheric dynamics that unfolded in nature including the occurrence or non-occurrence of ESF. The positive results indicate that the important processes underlying ESF have been taken into consideration in the modeling. Most importantly, the simulation has produced no "false alarms," meaning that no necessary conditions for ESF are being overlooked.

Sometimes, the numerical simulations fail to predict ESF depletions. We suspect that the cause of the depletions lies outside the immediate field of view of Jicamarca and outside the scope of our simulations. We have therefore built, programmed, and fielded a new kind of multistatic, software-defined HF radar/sounder/beacon system for observing the ionosphere regionally. The system uses HF signals to probe the ionosphere along multiple ground-to-ground ray paths. Complete knowledge of the state of the F region ionosphere would permit us to predict the main characteristics of the received HF signals (range and group delay, arrival bearing, amplitude, and polarization). Our objective has been to go the other way and to infer the regional ionospheric state from the totality of the beacon data. The ionospheric specification thus rendered should reveal the presence of nascent irregularities in the ionosphere that could precondition or "seed" it for ESF events. Such irregularities would constitute "sufficient conditions" for ESF not accounted for in our simulation studies.

Our beacon network now includes four stations – one transmitting station at Ancon, two receiving stations at Jicamarca, and one receiving station at Huancayo, Peru. The stations utilize two frequencies, doubling the number of ray paths otherwise available and increasing the span of altitudes being probed. Data from a campaign conducted in August of 2015 have been processed using a new, end-to-end inversion method. The method is able to reproduce the ionosphere which would give rise to the HF propagation paths observed while being minimally structured. While the method is computationally expensive, it is scalable and stable. The first results from the beacon network and the data inversion are presented.

Introduction

Under this award, we studied the aeronomy of the equatorial ionosphere under conditions known historically as "equatorial spread F" (ESF). ESF is space-weather phenomenon occurring mainly after sunset and characterized by towering plumes of depleted plasma that are striking to observe. ESF generates plasma density irregularities with relative amplitudes approaching 100% of background with scale sizes ranging from centimeters to hundreds of kilometers. ESF disrupts radio communication, navigation, and imaging systems including space-based synthetic aperture radars and over-the-horizon radars and therefore poses a hazard (see reviews by *Woodman* [2009] and *Kelley et al.* [2011]). We study ionospheric instability to mitigate the hazard.

Unlike ionospheric substorms in the auroral zone, ESF does not require solar storms and is not limited to periods of high geomagnetic activity. Spread F occurs frequently in the equatorial zone, more often than not in some seasons, and its impact varies with the season and solar cycle along with the level of geomagnetic activity. The instabilities responsible for ESF are variants of simple $E \times B$ instability and derive their free energy from the unstable stratification of the ionosphere after sunset. Despite this, ESF has proven to be difficult to predict. This is because its fundamental drivers, the background zonal ionospheric electric field and the thermospheric winds, are themselves highly variable. Paradoxically, the only time when ESF can be predicted reliably is during geomagnetically active periods when the background electric fields and winds have somewhat predictable storm-time responses.

The predominant circulation pattern in the postsunset equatorial ionosphere is vortex flow in the region where the zonal conductivity gradient from the evening terminator meets the vertical conductivity gradient in the steep postsunset bottomside density profile (e.g. *Haerendel et al.* [1992]; *Kudeki and Bhattacharyya* [1999]; *Eccles et al.* [1999]). Attendant with the vortex is vertical shear in the horizontal plasma flow [*Kudeki et al.*, 1981; *Tsunoda et al.*, 1981], and attendant with the shear is vertical current. While vertical current had not previously been considered in ESF studies, *Hysell and Kudeki* [2004] showed that it actually contributes substantially to ionospheric instability, reducing the e-folding time of growing irregularities and accounting for the preferred horizontal scale sizes seen on ESF morphology. In addition, instabilities driven by vertical currents can account for precursor "bottom-type" layers which are nearly ubiquitous in the postsunset equatorial ionosphere and inhabit the valley region where instabilities driven by zonal currents should not function.

Under our award from AFOSR, we have been testing whether the balance of the physics controlling the stability of the postsunset equatorial ionosphere and the onset of ESF was well understood in view of the new ideas about shear flow and vertical currents. Our research has had four phases. In the first, we developed a three-dimensional numerical simulation of the equatorial ionosphere capable of reproducing both realistic background ionospheric flows and fast-growing irregularities. The emphasis was on reproducing vertical currents and their effects. In the second, we developed an experimental mode at the Jicamarca Radio Observatory capable of observing the most important drivers of ESF at once while also being able to observe its effects. Jicamarca makes direct observations of vector plasma drifts, and three Fabry-Perot interferometers have recently become available for measuring horizontal thermospheric winds which help drive the evening vortex. Third, we conducted a number of campaigns at Jicamarca. We used the resulting data to both initialize and force the numerical simulation and then investigated whether the predictions it makes on given nights are accurate.

In the final phase of the project, we added a new experimental capability. We designed, programmed, and deployed a network of HF beacons. The beacons employ software-defined transceivers and function as next-generation multistatic HF sounders. By employing PRN coding and other innovations, the sounders can measure phase and group delay, amplitude, polarization, and arrival angles of the signals reflected from the ionosphere. The sounders operate at very low power levels and are inexpensive to purchase, deploy, and operate. The network now includes a transmitting station in Ancon, Peru, and receiving stations at Jicamarca (2) and Huancayo (1).

The HF beacon network probes the bottomside F region ionosphere in the region around Jicamarca, providing information about plasma density irregularities well outside the radar's field of view (that might eventually drift into the field of view). The advantage of the beacon network is that it can monitor a large volume of space for extended periods of time at low cost and with only minimal human intervention, infrastructure, and impact. The disadvantage is that the observables are related to the ionospheric state in a complicated way. Like GPS signals, the beacon signals represent path-integrated quantities. Unlike GPS, the paths in this case are not straight lines and are unknown a priori. Furthermore, the HF beacon observables depend on parameters other than the plasma number density (the magnetic field and the electron-neutral collision frequency notably) and in a complicated way. Inverting the beacon data is challenging, but the computational resources required are now in place.

The software required to invert the beacon data and reconstitute a model ionosphere on their basis is nontrivial, to say the least, The problem is underdetermined and poorly conditioned (potentially unstable). We developed an algorithm for this purpose that is practical if computationally expensive. The algorithm employs raytracing to solve for rays emanating from a beacon transmitter as an initial value problem. The raytracing code is the inner iterative loop of the algorithm. The middle iterative loop is a shooting algorithm that assures that the rays launched from transmitting stations are received at receiving stations, thus turning the problem into a boundary value problem. The observables (group delay, phase delay, amplitude, bearing on reception) for every ray between every station pair at every HF frequency is thus predicted for a candidate model ionosphere.

In the outer loop of the algorithm, the parameters that describe the model ionosphere are updated so as to make the predicted and observed observable match. This is an optimization problem which we solve using a damped Levenberg Marquardt method. Damping is required to stabilize the results. Other data sources including electron density profiles from Jicamarca and elsewhere can easily be incorporated in the inversion. The model itself is parametrized using a 3-parameter Chapman function to describe vertical variations in electron number density and bicubic B-splines to describe horizontal variations. In all, our model ionosphere is parametrized in terms of 675 coefficients (an adjustable number). Empirical models are used to describe the background neutral atmosphere, ionospheric composition, and geomagnetic field. These quantities are necessary for calculating the complex wave index of refraction along the ray paths.

The algorithm was demonstrated using campaign data from August, 2015.

Accomplishments

The main accomplishments of our project during its first year are itemized below:

▷ Multiple ESF campaigns have been conducted at Jicamarca. The list of campaigns now reads

as:

Dec. 17–21, 2012 (N_e, T_e, T_i, $\mathbf{v}_\perp$ profiles + radar RTI)

Apr. 11–16, 2013 (added FPI winds)

Sep. 16 – Oct. 3, 2013 (added wide-field imaging)

May 5–9, 2014 (added 2 HF stations)

Nov. 24 – 28, 2014

Dec. 15 – 22, 2014

Feb. 9 – 15, 2015

Mar. 23 – 27, 2015

Aug. 25 – 28, 2015 (added 3rd HF station)

Dec. 9 –13, 2015

Data from all of the campaigns prior to Dec. 2015 have been reduced and analyzed. The most recent campaign data are undergoing analysis.

- ▷ The Cornell ionospheric simulation code was upgraded in a number of respects, including the addition of hydrogen ions and allowances for the effects of ion inertia. The code was modified so as to be able to ingest data (in the form of initial conditions and drivers) from the Jicamarca ISR along with regional Fabry-Perot interferometers in Peru.
- ▷ A new observing mode was developed at Jicamarca for this project. Throughout its history, Jicamarca was used to observe ionospheric plasma density, temperature and composition or vertical and east-west drift profiles, but not both. The new mode subdivides the antenna array and incorporates time-division multiplexing to allow multiple observing modes to be run concurrently. Additionally, radar imaging of coherent scatter from ESF irregularities can be measured simultaneously. The new mode was employed in the AFOSR observing campaigns.
- ▷ The code was initialized and driven using data from the aforementioned campaigns. Our goal was to determine whether or not the simulation code produced the same results as nature given the same initial conditions and forcing. To a considerable degree, they did. We regard this as a significant achievement which we endeavored to document in the published literature. The result implies that the aeronomy of the postsunset equatorial ionosphere is sufficiently well understood for forecasting (to the extent the drivers, the electric fields and winds, can be forecast). That the simulation code produced no false alarms (predictions of topside irregularities where none were observed) implies that there is no hidden necessary conditions for ESF being overlooked.
- ▷ That the simulation results included some missed detections (observations of topside ESF plumes where none were predicted) suggests that there could be hidden sufficient conditions for ESF to occur. To test whether disturbances propagating into the region from outside are causing irregularities where none are expected, an HF beacon network for regional monitoring was developed.
- ▷ The HF beacon network was deployed and is now functioning. A signal chain for acquiring data, processing, and ingesting them into a regional ionospheric model based in statistical inverse theory has also been completed.
- ▷ The aforementioned work has been performed by the PI, Hysell, graduate students at Cornell, colleagues at Jicamarca, and with the help of Juha Vierinen, a former Jicamarca summer scholar

now employed at MIT Haystack Observatory. Results from our work has been presented at CEDAR workshops, at the ISEA meeting in Ethiopia, and at the recent Multistatic Meteor Radar workshop at IAP in Germany.

- ▷ Four papers describing our work have been published:
  - ◦ Hysell, D. L., R. Jafari, M. A. Milla, and J. W. Meriwether (2014), Data-driven numerical simulations of equatorial spread F in the Peruvian sector, J. Geophys. Res. Space Physics, 119, 38153827, doi:10.1002/2014JA019889.
  - ◦ Hysell, D. L., M. A. Milla, L. Condori, and J. W. Meriwether (2014), Data-driven numerical simulations of equatorial spread F in the Peruvian sector: 2. Autumnal equinox, J. Geophys. Res. Space Physics, 119, 69816993, doi:10.1002/2014JA020345.
  - ◦ Hysell, D. L., M. A. Milla, L. Condori, and J. Vierinen (2015), Data-driven numerical simulations of equatorial spread F in the Peruvian sector 3: Solstice, J. Geophys. Res. Space Physics, 120, 10,809ŏ201310,822, doi:10.1002/2015JA021877.
  - ◦ Hysell, D. L., M. A. Milla, and J. Vierinen (2016), A multistatic HF beacon network for ionospheric specification in the Peruvian sector, Radio Sci., 51, 392ŏ2013401, doi:10.1002/2016RS005951.

Narrative

Here, we show one of the many examples of model/data congruity arising from this study. The publication record gives a more complete accounting of model/data comparisons and their implications.

Fig. 1 shows observations made at Jicamarca during June-solstice conditions which are generally unfavorable for ESF. We were fortunate to have captured even one active ESF event in late April. This time, a bottom-type scattering layer appeared at 0010 UT (1910 LT) followed by the passages of a high-altitude radar plume beginning at about 0045 UT (1945 LT). In nature and in simulation, such layers are telltale of vertical currents which drive fast-growing irregularities in the bottomside and are prone to initiate topside ESF.

The plasma irregularities produced radar clutter and contaminated the incoherent scatter data, causing gaps in the record at certain altitudes and times. It was nonetheless possible to measure an uncontaminated electron density profile at 2330 UT (1830 LT) as well as the time history of the average vertical plasma drifts. The vertical drifts were very large on this night, reaching almost 50 m/s at 2330 UT, and remained upward through about 0100 UT (2000 LT) or about an hour longer than on the following evening when no ESF occurred. The unseasonably strong and sustained upward drifts were undoubtedly responsible for the high level of ESF activity.

Our numerical simulation draws initial and background parameters from a combination of empirical models tuned to reflect day-to-day variability in the campaign data. We use the PIM model to initialize the electron number density throughout the simulation space. A model is necessary here because our simulation requires initialization over a broad span of locations and local times and not just the places and local times when measurements are available. We feed PIM a proxy value of the F10.7 solar flux index so that it predicts a number density profile which is congruent with the radar data at the start of the simulation. The initial ion composition is taken from the IRI-2007 model [*Bilitza and Reinisch*, 2008]. Neutral parameters necessary for calculating ion- and

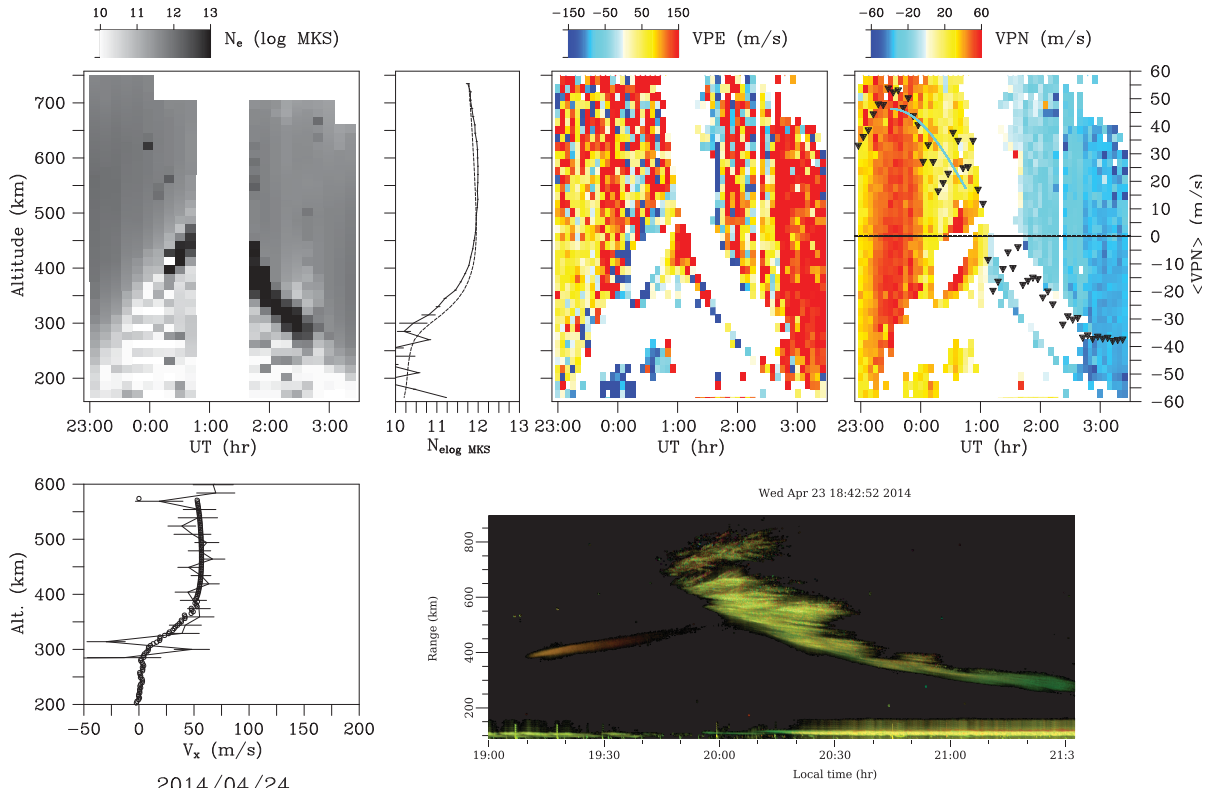

Figure 1: Jicamarca observations of ESF April 23/24, 2014. Top row, from left to right: electron density, electron density profiles at 2330 UT, zonal plasma drifts, and vertical plasma drifts. Bottom row left: Measured zonal plasma drift profiles at 2330 UT (solid line with error bars) together with the computed drift profile (plotted points) at the start of the numerical simulation. Bottom row right: coherent backscatter. Note that UT = LT + 5 hr.

after 25 min.

after 75 min.

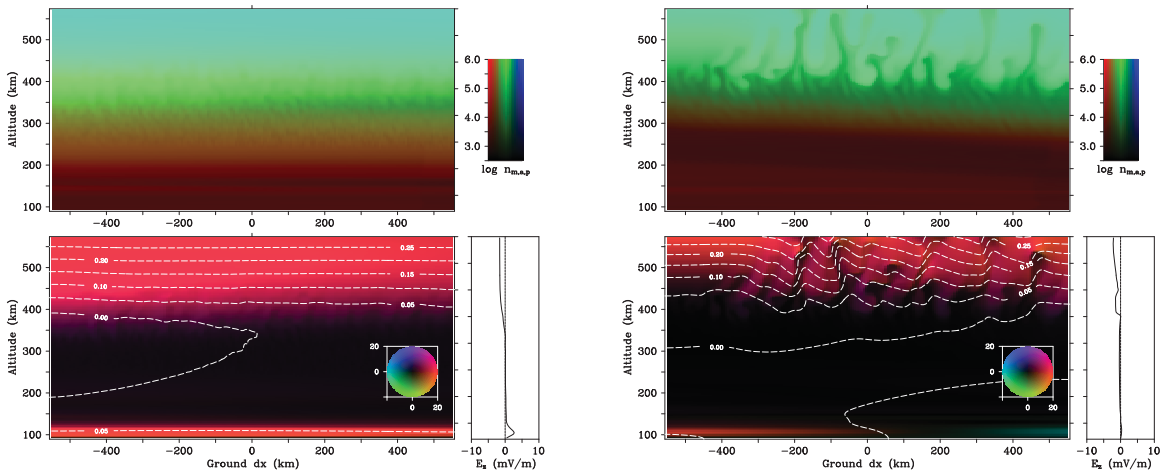

Figure 2: Numerical simulation of events on Apr. 23/24, 2014 initialized at 2330 UT. The panels on the left and right show simulated results after 25 and 75 min., respectively. The top panels show plasma number density, with red, green, and blue tones representing molecular, atomic, and protonic ion abundances, respectively. The Bottom panels indicate vector current density in the equatorial plane in nA/m^2 according to the circular legend shown. White lines are equipotentials, approximate streamlines of the flow. The vertical electric field through the midpoint of the simulation is plotted in profiles to the right of the current density plots. Note that diamagnetic currents have no effect on dynamics and are not included in the current densities shown.

electron-neutral collision frequencies are taken from the NRLMSISE-00 model [*Picone et al.*, 2002]. The neutral parameters from NRLMSISE-00 are updated dynamically throughout the simulation.

The background zonal electric field used in the simulation is specified according to the ISR vertical drifts measurements. Finally, the neutral winds in the simulation are provided by the new Horizontal Wind Model '14 (HWM14) model [*Drob et al.*, 2015]. The latest version of the HWM model was found to reproduce ground-based Fabry Perot interferometer data from the American sector much more accurately than older versions of the model. The model winds are rescaled in our simulations in order to account for day-to-day variability. Specifically, the zonal neutral winds are scaled by a single, constant factor meant to optimize congruity between the predicted and measured zonal plasma drift profiles at the initial time of simulations. (The meridional winds are imported but not scaled.) We refer to the multiplicative scaling constant below as s.

Fig. 2 shows simulation results for the high-activity event of the April, 2014, campaign. After 25 min., the F layer in the Apr. 23/24 simulation ascended noticeably farther than in the simulation for the following day, when no ESF plumes were predicted. The upward tilt in the layer from west

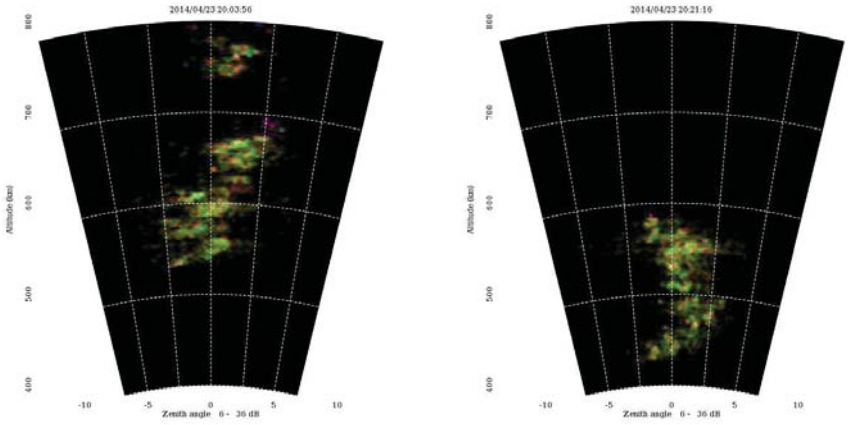

Figure 3: Aperture synthesis radar imagery for Apr. 23, 2014.

to east, from earlier to later local times, is an indicator of continuing, rapid ascent. After just 25 min., distinct plasma density irregularities formed in the strata between about 350–400 km altitude. This matches the height range where bottom-type layers emerged initially in the campaign data. This altitude range is also coincident with the region of vertical current which is signified by violet hues in the transverse current density panel.

By the 75-min. time step (0045 UT, 1945 LT), the *F* layer ascended further, and irregularities grew, developed, and ascended to altitude strata where the current was mainly eastward and strong. The irregularities penetrated into the topside and through the upper boundary of the simulation space in some cases. The simulation reproduced the topside plumes clearly evident in the campaign data which ascended to 700 km by 0045 UT (1945 LT) when they first drifted over the radar.

Radar images for two distinct radar plumes observed on April 23, 2014, are shown in Fig. 3. The images depict signal-to-noise ratio versus range and azimuth in the equatorial plane given an incoherent integration period of about 10 s. The signal-to-noise ratio is represented by the brightness of the pixels in the image in dB in the range indicated. The hue and saturation of the pixels reflect Doppler spectral information, but we make no attempt to interpret that information in this instance since most of the echoes are strongly frequency aliased. The resolution of the pixels is finer than 1 km x 1 km. Animated sequences of images (not shown) reveal that the irregularities in question are undergoing creation and destruction while moving in an inhomogeneous flow field, i.e., not simply frozen into a uniform background flow.

In previous experiments, we have found that backscatter at this spatial scale arrives from the most deeply depleted regions and channels within the irregularities and so delineate the gross irregularity structure [*Hysell et al.*, 2009]. There is therefore some basis for comparison between these images and the numerical simulations. However, coherent scatter signifies the presence of plasma density irregularities at the Bragg scale only and so the correspondence is imperfect at best.

The radar plumes in Fig. 3 are typical of ESF, manifesting backward "C" shapes, narrow

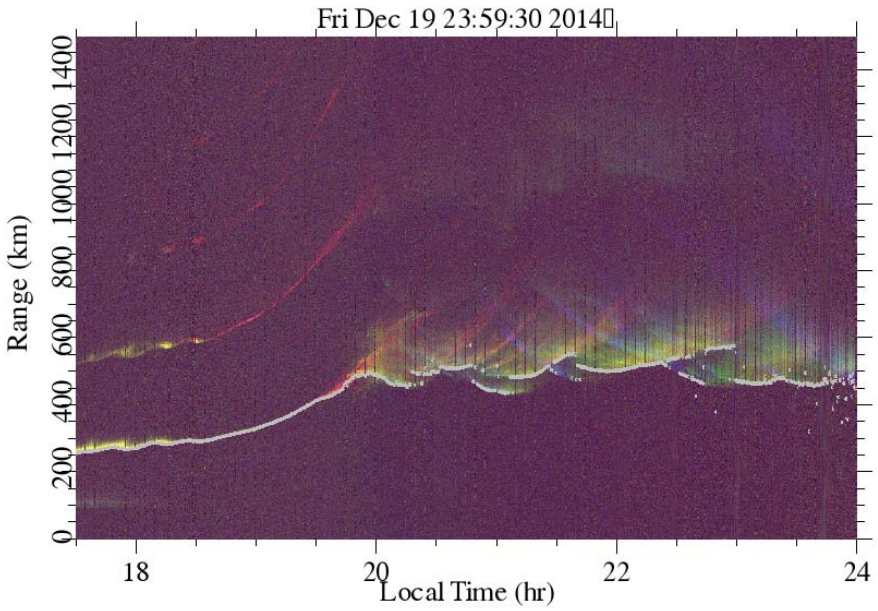

Figure 4: Data from a single HF beacon link (Ancon-Jicamarca) at a single frequency. The figure shows received power versus time and group range. The brightness of each pixel indicates SNR, and the hue indicates Doppler shift. White plotter symbols indicate the group range of the first-hop echo. These are the primary data used by our ionospheric recovery method at present. Amplitude, Doppler shift, and arrival bearing are other observables that can eventually be utilized for ionospheric recovery.

vertical channels, and a high degree of structuring indicating secondary interchange instability driven mainly by zonal winds. The plumes exhibit modest tilts from the vertical and occasionally bifurcate. The width of the imaged region is approximately 100 km at 600-km altitude which is sufficient to contain one or sometimes two different plumes. Comparison with Fig. 2 reveals these characteristics to be shared by the radar plumes that develop in simulation.

We turn now to our HF-beacon work which is necessary to expand the regional coverage around the Jicamarca radar and to help account for the events we sometimes observe which defy simulation predictions in being overly active. Figure 4 shows representative data for the Ancon-Jicamarca HF link for an evening during one of our campaigns when ESF occurred. The figure shows echo power versus group range and local time. The brightness of each pixel denotes the signal-to-noise ratio, and the hue denotes the Doppler shift, with red (blue) tones indicating red (blue) shifts. White plotter symbols are the result of an algorithm which attempts to find the virtual height of the first hop. These are presently the primary data used for ionospheric reconstruction.

The figure shows that the bottomside of the ionosphere rose quickly between 1800–2000 LT. Some small but distinct wavelike perturbations were present prior to about 1845 LT, but the trace was fairly smooth thereafter. This particular dataset does not indicate obvious ESF precursors or "sufficient conditions."

Group-delay estimates for all four links have been combined with ISR-derived density profiles from Jicamarca and modeled according to the methodology described briefly above. The results for observations of Aug. 25, 2015, are shown in Figure 5. Six panels depict results for four local times prior to the passage of the radar plume. Quasi-isodensity contours for $n_e = 5 \times 10^4$ cm^3 and $n_e = 5 \times 10^5$ cm^3 are indicated in each panel by the green and cyan surfaces, respectively. The isodensity surfaces are found to be nearly horizontal planes in the interval shown. In order to emphasize differences from pure horizontal stratification, the surfaces actually show the average height plus the deviation from the average multiplied by a factor of five.

The ionospheric reconstruction captures the gradual postsunset ascent of the *F* layer over time as well as the east-west ionospheric tilt that follows the passage of the solar terminator. Animated sequences of figures like those in Figure 5 also suggest subtle ionospheric structuring at the spatial and temporal scales being analyzed. The number of links is too few to specify whether features are propagating or advecting through the region, however.

Significantly, perturbations in the group delays of the four links are accounted for by the model not through wholesale layer ascent and descent but instead mainly through layer tilts. A tilted ionosphere forces the rays to propagate away from great-circle paths. Very subtle tilts can induce significant changes in group delay this way. It is therefore incorrect to interpret group delay as a proxy measurement for layer height at the reflection point. The modeled layer height barely changes on time scales during which the measured group delays vary significantly.

Future challenges

One of the main challenges at this point is finding a way to render the ionospheric specification in such a way that details are more apparent. Volumetric rendering of scientific data is still an unsolved problem. Another problem involves data fusion and the combination of the beacon project with the aforementioned ISR campaigns and numerical simulations.

Quite a few improvements to the data inversion method can be made. One is the generalization of the altitude model to include both an *E*-region and and *F*-region Chapman layer. Such a model would be better at representing the plasma density in the valley region where the density can be uniform over broad altitude spans. Another is parallelization, which will be necessary as the number of links is increased. As each link can be traced individually, parallelization should be efficient.

In the future, it should also be possible to utilize more of the observables in the data inversion. The ray tracing code predicts the phase delay, power, and bearing of the received O- and X-mode signals already. Measured Doppler shifts prescribe the time rate of change of the phase delay from one timestep to the next. Discrepancies between the observables and the model prescriptions can readily be added to the objective function used in the outer loop if the inverse method.

Still other observables are available from the HF signals, although their utility to the project is less certain and requires investigation. It should be possible to observe the Faraday rotation of the signals received at Jicamarca. This is another indication of the line-integrated electron number

density. Like the phase delay, the Faraday angle is a modulo-two-pi quantity that is best used to constrain the time evolution of the ionosphere. Both the Faraday angle and the phase delay are continuous quantities, unlike the group delay which is quantized at the level of the range resolution of the beacon system. The precision is therefore potentially greater.

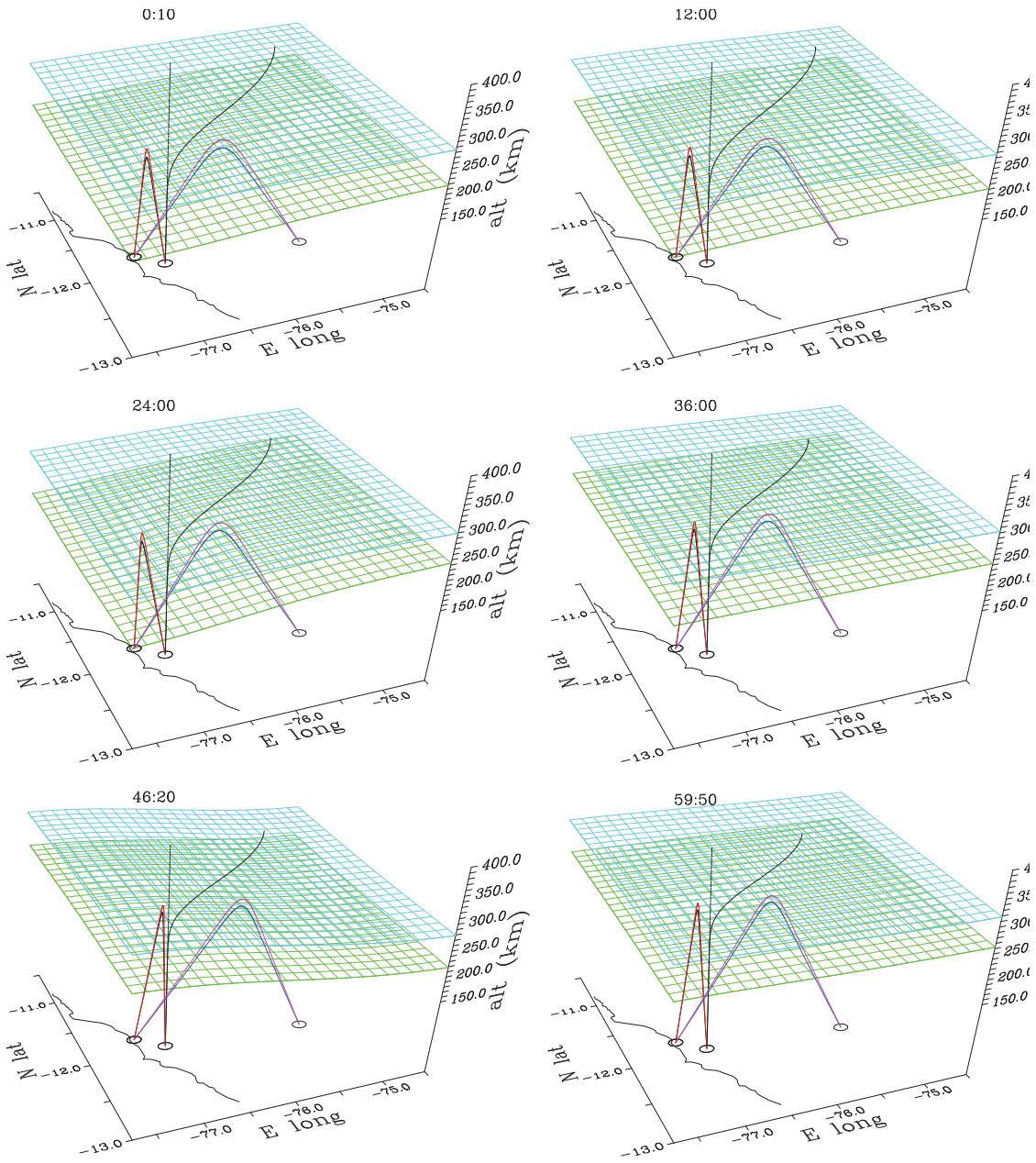

Figure 5: Ionospheric reconstructions based on beacon and ISR data. The six panels correspond to six different local times, as indicated. The ragged line in each panel is the Pacific coastline. The plotted surfaces are two isodensity contours. The black profile is the model density profile evaluated over Jicamarca. The four rays represent the four HF beacon links. The underlying ionospheric model is consistent with all available data at the given time.

Bibliography

Bilitza, D., and B. W. Reinisch, International Reference Ionosphere 2007: Improvements and new parameters, *Adv. Space Res.*, *42*, 599–609, 2008.

Drob, D. P., et al., An update to the Horizontal Wind Model (HWM): The quiet time thermosphere, *Earth and Space Science*, *2*, doi:10.1002/2014EA000,089, 2015.

Eccles, J. V., N. Maynard, and G. Wilson, Study of the evening drift vortex in the low-latitude ionosphere using San Marco electric field measurements, *J. Geophys. Res.*, *104*, 28,133, 1999.

Haerendel, G., J. V. Eccles, and S. Cakir, Theory for modeling the equatorial evening ionosphere and the origin of the shear in the horizontal plasma flow, *J. Geophys. Res.*, *97*, 1209, 1992.

Hysell, D. L., and E. Kudeki, Collisional shear instability in the eqautorial *F* region ionosphere, *J. Geophys. Res.*, *109*, (A11,301), 2004.

Hysell, D. L., R. B. Hedden, J. L. Chau, F. R. Galindo, P. A. Roddy, and R. F. Pfaff, Comparing *F* region ionospheric irregularity observations from C/NOFS and Jicamarca, *Geophys. Res. Lett.*, *36, L00C01*, doi:10.1029/2009GL038,983, 2009.

Kelley, M. C., J. J. Makela, O. de la Beaujardiere, and J. Retterer, Convective ionospheric storms: A review, *Rev. Geophys.*, *49*, doi:10.1029/2010RG000,340, 2011.

Kudeki, E., and S. Bhattacharyya, Post-sunset vortex in equatorial *F*-region plasma drifts and implications for bottomside spread-*F*, *J. Geophys. Res.*, *104*, 28,163, 1999.

Kudeki, E., B. G. Fejer, D. T. Farley, and H. M. Ierkic, Interferometer studies of equatorial *F* region irregularities and drifts, *Geophys. Res. Lett.*, *8*, 377, 1981.

Picone, J. M., A. E. Hedin, D. P. Drob, and A. C. Aikin, NRLMSISE-00 empirical model of the atmosphere: Statistical comparisons and scientific issues, *J. Geophys. Res.*, *107, A12*, doi: 10.1029/2002JA009,430, 2002.

Tsunoda, R. T., R. C. Livingston, and C. L. Rino, Evidence of a velocity shear in bulk plasma motion associated with the post-sunset rise of the equatorial *F* layer, *Geophys. Res. Lett.*, *8*, 807, 1981.

Woodman, R. F., Spread F- An old equatorial aeronomy problem finally resolved?, *Ann. Geophys.*, *27*, 1915–1934, 2009.

1.

1. Report Type

Final Report

Primary Contact E-mail

Contact email if there is a problem with the report.

dlh37@cornell.edu

Primary Contact Phone Number

Contact phone number if there is a problem with the report

607-255-0630

Organization / Institution name

Cornell University

Grant/Contract Title

The full title of the funded effort.

Three-Dimensional Simulations of Ionospheric Plasma Irregularities and Forecast Studies of Equatorial Spread F

Grant/Contract Number

AFOSR assigned control number. It must begin with "FA9550" or "F49620" or "FA2386".

FA9550-12-1-0462

Principal Investigator Name

The full name of the principal investigator on the grant or contract.

David Hysell

Program Manager

The AFOSR Program Manager currently assigned to the award

Julie Moses

Reporting Period Start Date

09/15/2015

Reporting Period End Date

09/14/2016

Abstract

Progress simulating equatorial spread F (ESF) in pursuit of a space-weather forecast capability is summarized. ESF is the main manifestation of space weather at low magnetic latitudes in the ionosphere and is responsible for disrupting communication, navigation, imaging, and surveillance systems important to the Air Force and other federal agencies.

A 3D numerical simulation of the plasma instabilities responsible for ESF written at Cornell has been developed and upgraded under this award. Plasma number density, electric field, and neutral wind data necessary for driving the simulation have been collected in campaigns at the Jicamarca Radio Observatory conducted approximately semi-annually. The simulation code is initialized and forced using campaign data. Simulation results, specifically the plasma depletions and plumes characteristic of ESF, are compared with coherent scatter radar imagery of ESF irregularities made at Jicamarca. Such imagery is directly comparable to the 3D simulation products, offering a prediction-assessment strategy that is uniquely conducive to closure. In multiple campaign studies, the simulation was able to recover the ionospheric dynamics that unfolded in nature including the occurrence or non-occurrence of ESF. The positive results indicate that the important processes underlying ESF have been taken into consideration in the modelling.

Most importantly, the simulation has produced no ``false alarms," meaning that no necessary conditions for ESF are being overlooked.

Sometimes, the numerical simulations fail to predict ESF depletions. We suspect that the cause of the depletions lies outside the immediate field of view of Jicamarca and outside the scope of our simulations We have therefore built, programmed, and fielded a new kind of multistatic, software-defined HF radar/sounder/beacon system for observing the ionosphere regionally. The system uses HF signals to probe the ionosphere along multiple ground-to-ground ray paths. Complete knowledge of the state of the F region ionosphere would permit us to predict the main characteristics of the received HF signals (range and group delay, arrival bearing, amplitude, and polarization). Our objective has been to go the other way and to infer the regional ionospheric state from the totality of the beacon data. The ionospheric specification thus rendered should reveal the presence of nascent irregularities in the ionosphere that could precondition or ``seed" it for ESF events. Such irregularities would constitute ``sufficient conditions" for ESF not accounted for in our simulation studies.

Our beacon network now includes four stations -- one transmitting station at Ancon, two receiving stations at Jicamarca, and one receiving station at Huancayo, Peru. The stations utilize two frequencies, doubling the number of ray paths otherwise available and increasing the span of altitudes being probed. Data from a campaign conducted in August of 2015 have been processed using a new, end-to-end inversion method. The method is able to reproduce the ionosphere which would give rise to the HF propagation paths observed while being minimally structured. While the method is computationally expensive, it is scalable and stable. The first results from the beacon network and the data inversion are presented.

Distribution Statement

This is block 12 on the SF298 form.

Distribution A - Approved for Public Release

Explanation for Distribution Statement

If this is not approved for public release, please provide a short explanation. E.g., contains proprietary information.

SF298 Form

Please attach your SF298 form. A blank SF298 can be found here. Please do not password protect or secure the PDF The maximum file size for an SF298 is 50MB.

AFD-070820-035.pdf

Upload the Report Document. File must be a PDF. Please do not password protect or secure the PDF . The maximum file size for the Report Document is 50MB.

afosr_f.pdf

Upload a Report Document, if any. The maximum file size for the Report Document is 50MB.

Archival Publications (published) during reporting period:

Hysell, D. L., R. Jafari, M. A. Milla, and J. W. Meriwether (2014), Data-driven numerical simulations of equatorial spread F in the Peruvian sector, J. Geophys. Res. Space Physics, 119, 3815â3827, doi:10.1002/2014JA019889.

Hysell, D. L., M. A. Milla, L. Condori, and J. W. Meriwether (2014), Data-driven numerical simulations of equatorial spread F in the Peruvian sector: 2. Autumnal equinox, J. Geophys. Res. Space Physics, 119, 6981â6993, doi:10.1002/2014JA020345.

Hysell, D. L., M. A. Milla, L. Condori, and J. Vierinen (2015), Data-driven numerical simulations of equatorial spread F in the Peruvian sector 3: Solstice, J. Geophys. Res. Space Physics, 120, 10,809\u201310,822, doi:10.1002/2015JA021877.

Hysell, D. L., M. A. Milla, and J. Vierinen (2016), A multistatic HF beacon network for ionospheric

specification in the Peruvian sector, Radio Sci., 51, 392\u2013401, doi:10.1002/2016RS005951.

2. New discoveries, inventions, or patent disclosures:

Do you have any discoveries, inventions, or patent disclosures to report for this period?

No

Please describe and include any notable dates

Do you plan to pursue a claim for personal or organizational intellectual property?

Changes in research objectives (if any):

Change in AFOSR Program Manager, if any:

Kent Miller retired as the manager of this program and was replaced by Julie Moses during the award.

Extensions granted or milestones slipped, if any:

This project was granted a no-cost extension which has been completed.

AFOSR LRIR Number

LRIR Title

Reporting Period

Laboratory Task Manager

Program Officer

Research Objectives

Technical Summary

Funding Summary by Cost Category (by FY, $K)

	Starting FY	FY+1	FY+2
Salary			
Equipment/Facilities			
Supplies			
Total			

Report Document

Report Document - Text Analysis

Report Document - Text Analysis

Appendix Documents

2. Thank You

E-mail user

Jul 13, 2016 11:52:40 Success: Email Sent to: dlh37@cornell.edu